Dynamic Fault Weakening and Strengthening by Gouge Compaction and Dilatancy in a Fluid-Saturated Fault Zone

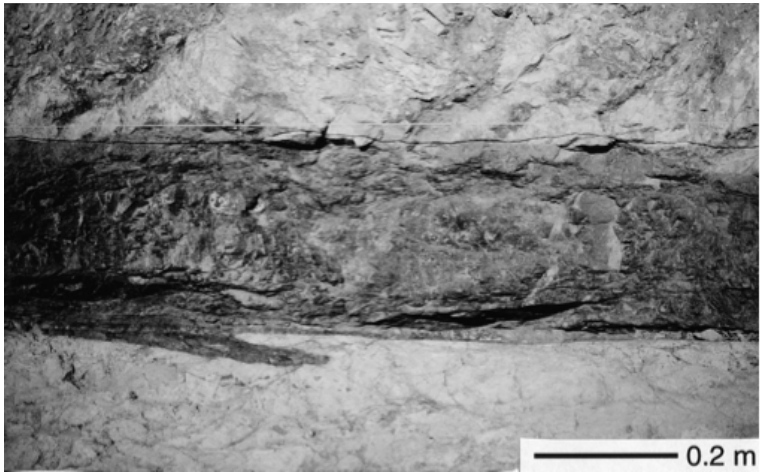

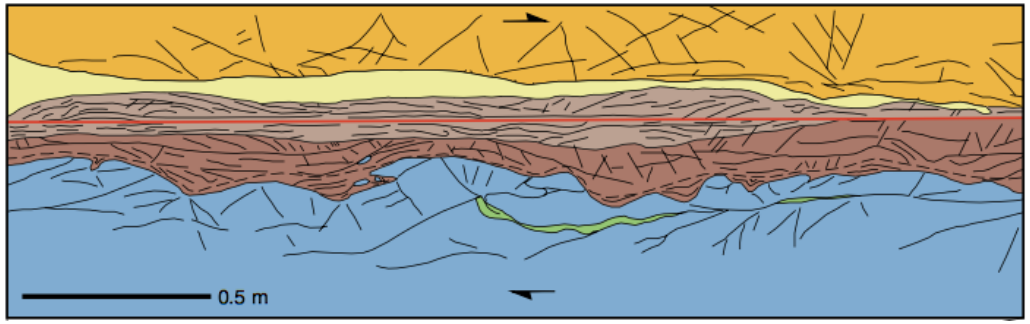

Evan Hirakawa and Shuo Ma

March 11, 2016

SCEC Rupture Dynamics Code Validation Workshop

Stress and heat-flow paradox for San Andreas Fault

- Observations indicate that SAF is weak
- Indicates friction coefficient of ~0.1 – 0.2
- Byerlee's Law: static friction should be around 0.6 – 0.85

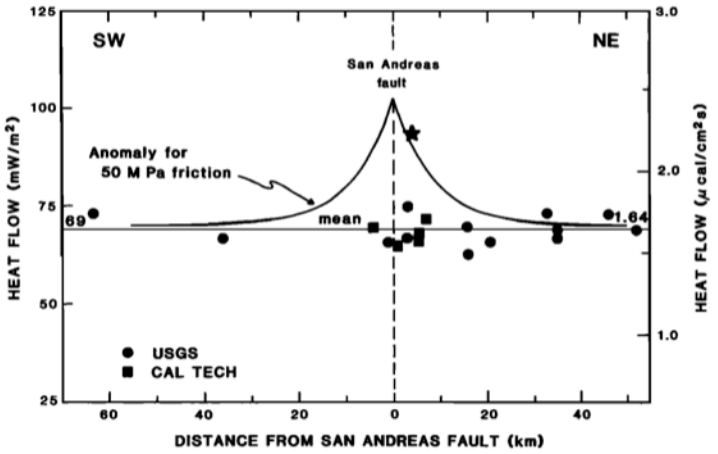

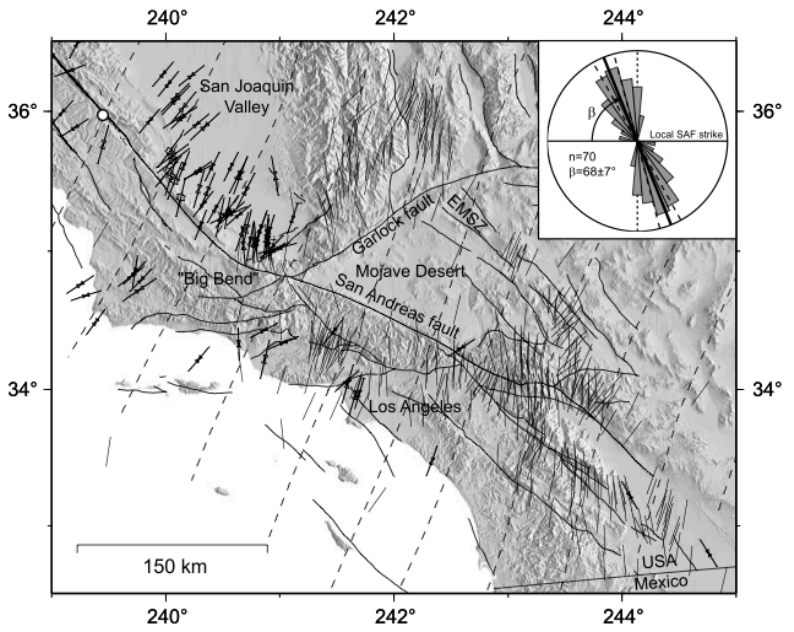

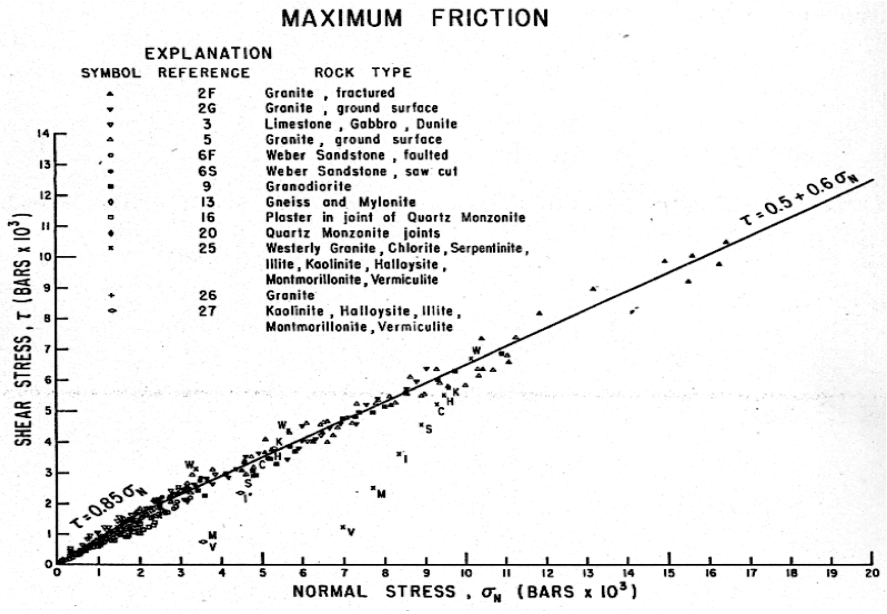

Why is the SAF weak?

Statically weak?

- Anomalous low-friction materials (e.g. clays)
- Permanently elevated pore pressure

Statically strong but dynamically weak?

- Flash heating of microscopic asperity contacts
- Thermal pressurization of fluids
- Acoustic fluidization
- Elastohydrodynamic lubrication
- Silica gel formation

See a critical review by Scholz (2006)

A Possible Drawback of Current Dynamic Weakening Mechanisms

"They offer no mechanism by which the static friction can be reduced." -- Scholz (2006)

- All mechanisms require slip to occur
- ~100 MPa strength drop (static friction minus dynamic friction) is inevitable.
- Leads to huge slip velocities (~300 m/s) and fault-parallel strain (~0.1)

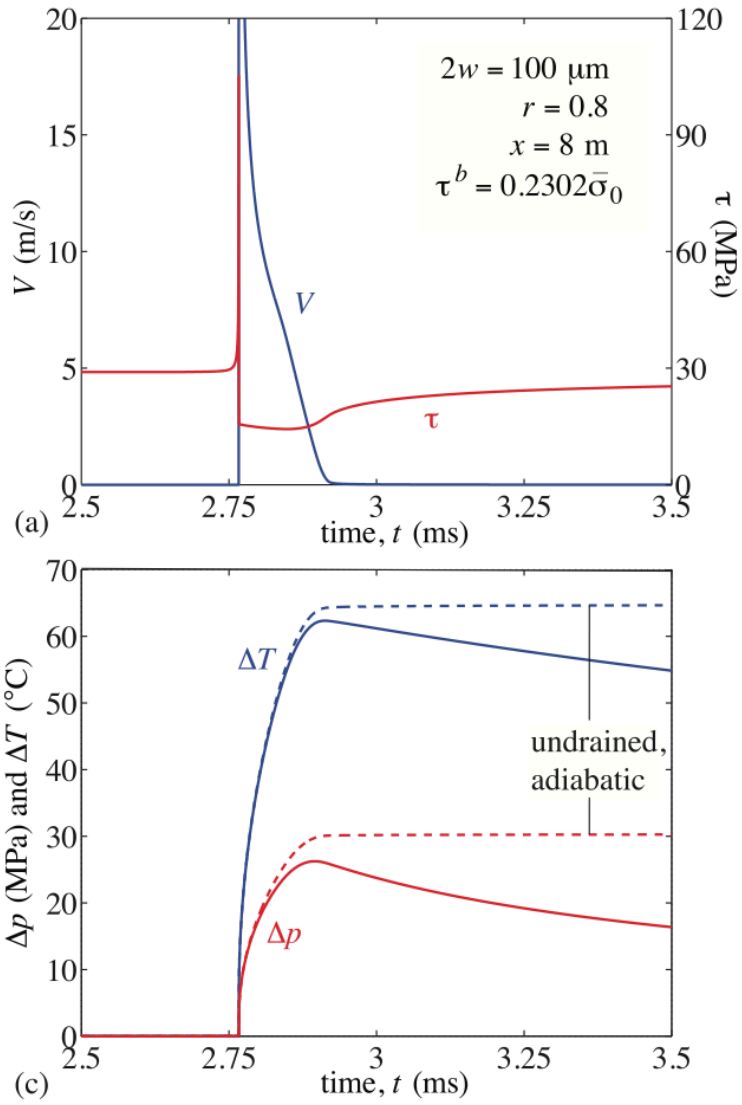

Noda, Dunham, and Rice (JGR, 2009)

Simulations with Off-Fault Plasticity

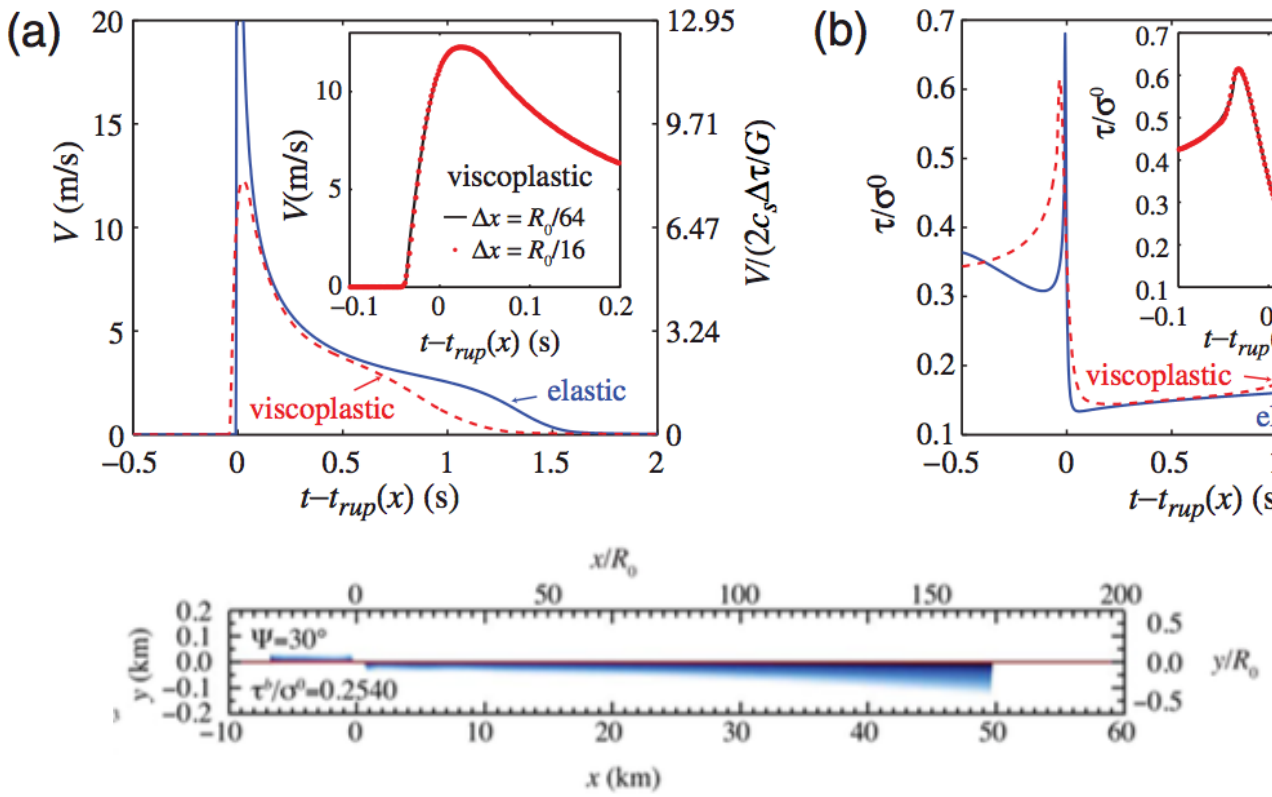

Dunham et al. (2011)

- Used Drucker-Prager plasticity
- Peak slip velocities drop to ~10 m/s with plasticity.
- But it is harder to drive rupture at low shear stress

Generic structure, mature fault zones:

F. Chester, J. Evans and R. Biegel, *J. Geoph. Res.*, **98** (B1), 771-786 (1993)

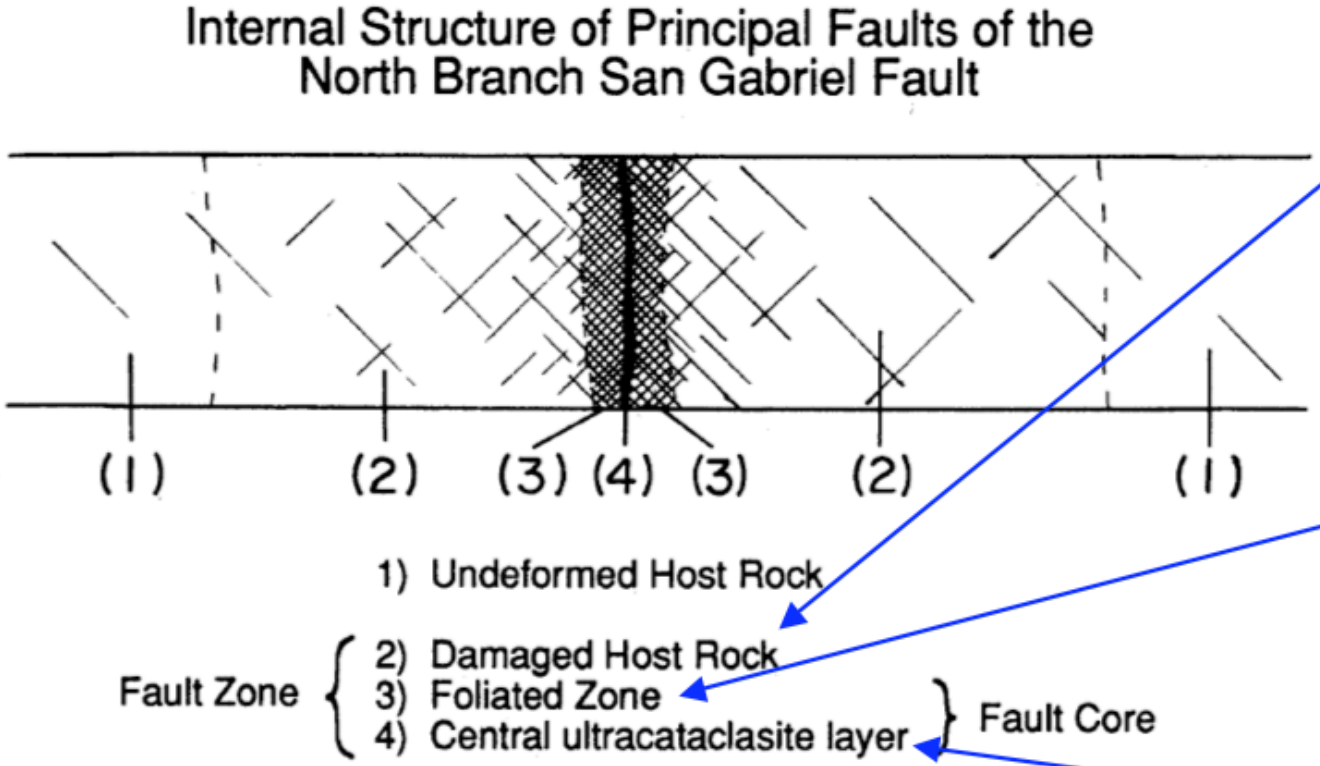

Fig. 2. Schematic section across the North Branch San Gabriel fault zone illustrating position of the structural zones of the fault. The diagram is not to scale.

30-100 m
(Damage ≈ *highly cracked rock.* Zone with macro faults or fractures extends ~ 10x further.)

1-10 m
(Sometimes described as *foliated gouge*, or for some faults, simply as *gouge*.)

10s-100s mm
(But ***principal failure surface*** can be *much thinner*, typically < 1-5 mm!)

Slide from Jim Rice

What about the gouge?

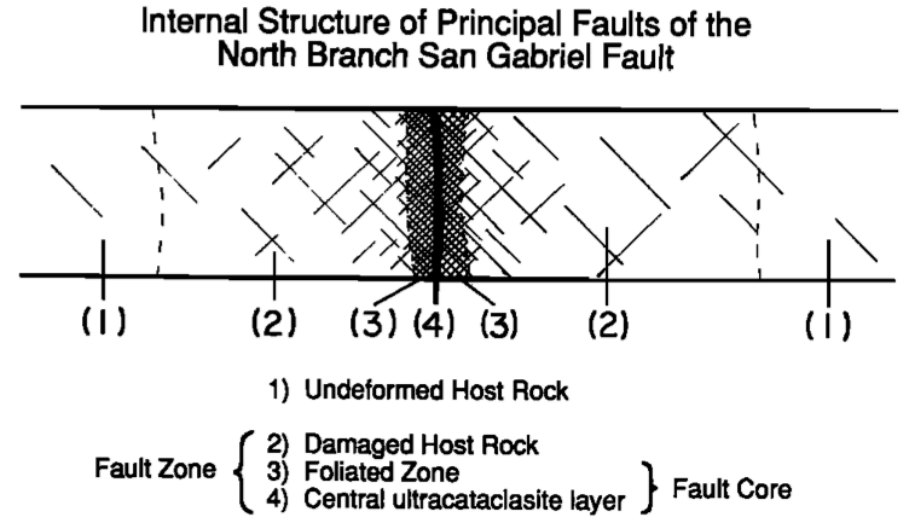

Fig. 2. Schematic section across the North Branch San Gabriel fault zone illustrating position of the structural zones of the fault. The diagram is not to scale.

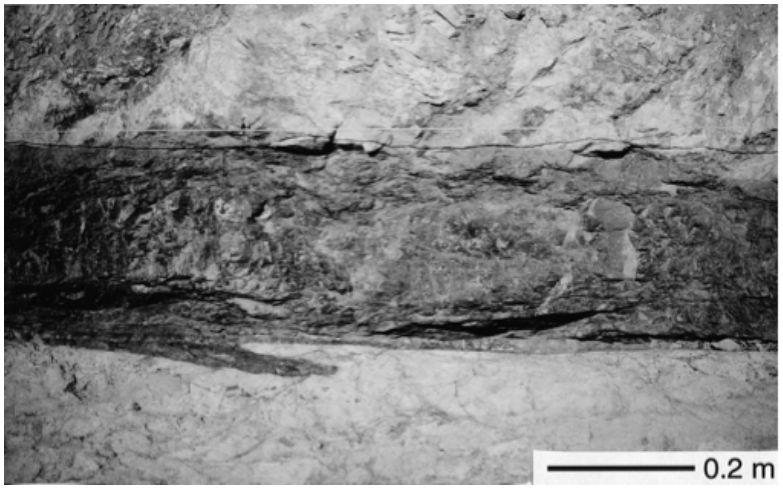

" … a more complete understanding of the earthquake process will probably require measurements of the permeability of fault zone materials, the width of the active shear zone, and studies of fault gouge dynamics."

Lachenbruch (1980)

Mechanical Characteristics of Fault Gouge

The damage zone rocks experience brittle failure
The gouge readily compacts and deforms more ductilely

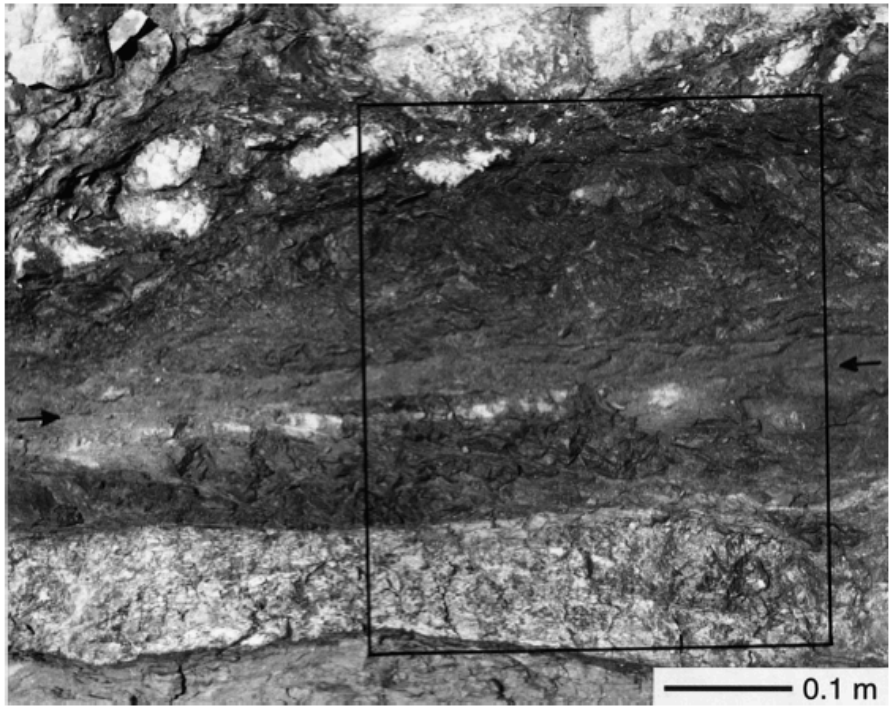

Chester and Chester (1998)

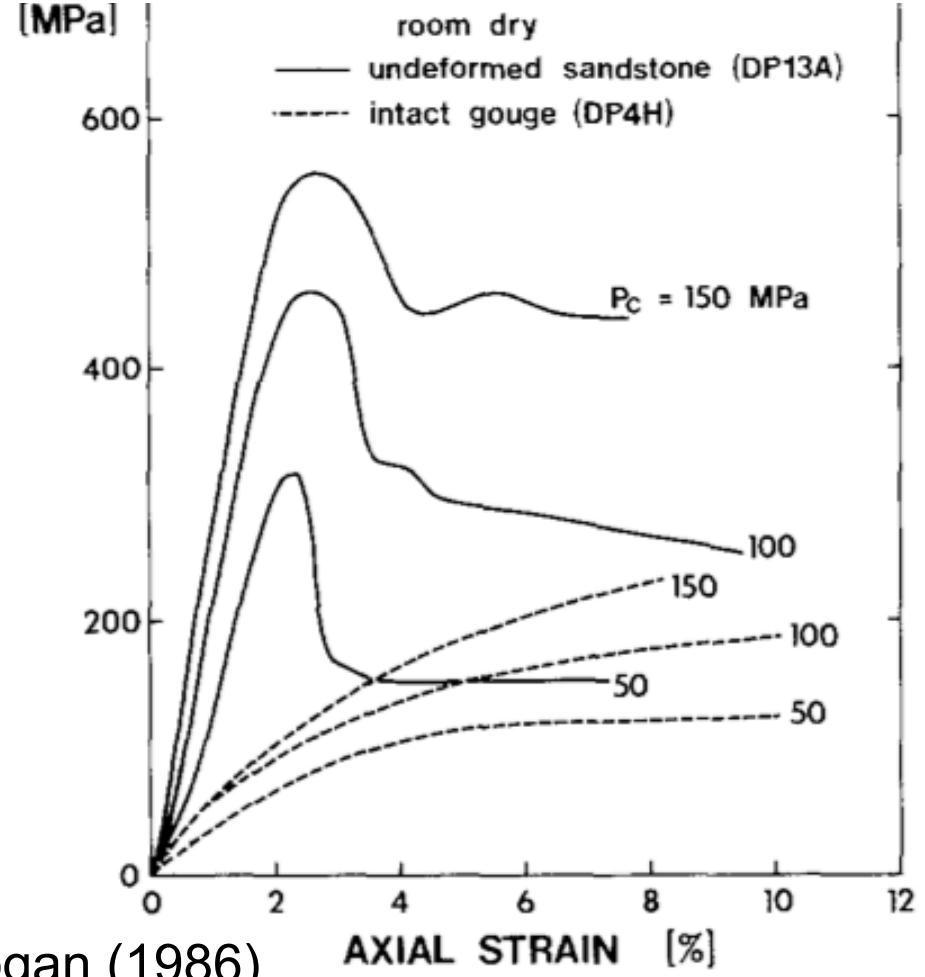

Chester and Logan (1986)

Creep, compaction and the weak rheology of major faults

Norman H. Sleep* **& Michael L. Blanpied†**

* Department of Geophysics, Stanford University, Stanford, California 94305, USA
† United States Geological Survey, Mail Stop 977, Menlo Park, California 94025, USA

Nature (1992)

Field and laboratory observations suggest that the porosity within fault zones varies over earthquake cycles so that fluid pressure is in long-term equilibrium with hydrostatic fluid pressure in the country rock. Between earthquakes, ductile creep compacts the fault zone, increasing fluid pressure, and finally allowing frictional failure at relatively low shear stress. Earthquake faulting restores porosity and decreases fluid pressure to below hydrostatic. This mechanism may explain why major faults, such as the San Andreas system, are weak.

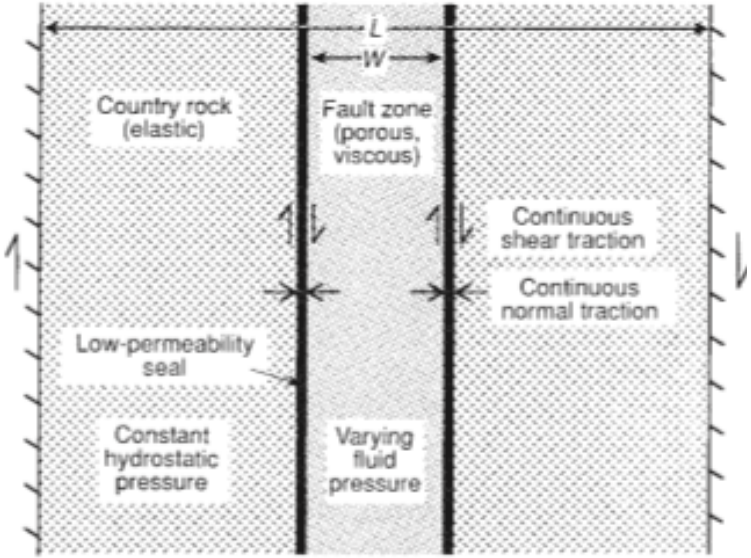

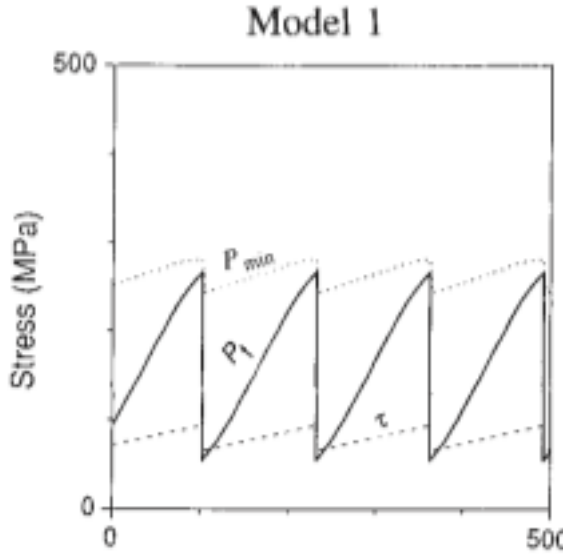

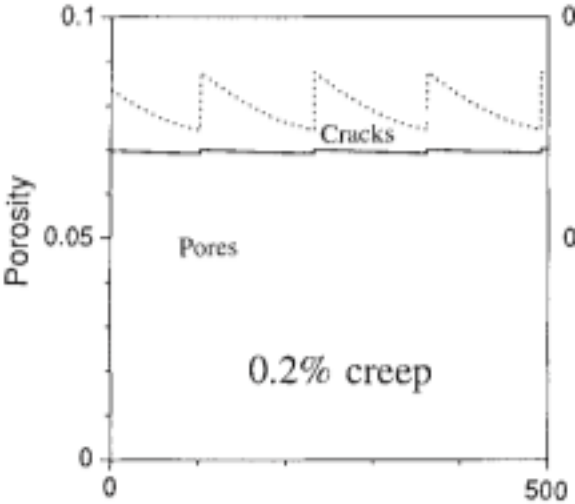

Gouge behavior in a dynamic rupture model?

Two-Phase Undrained Gouge Deformation

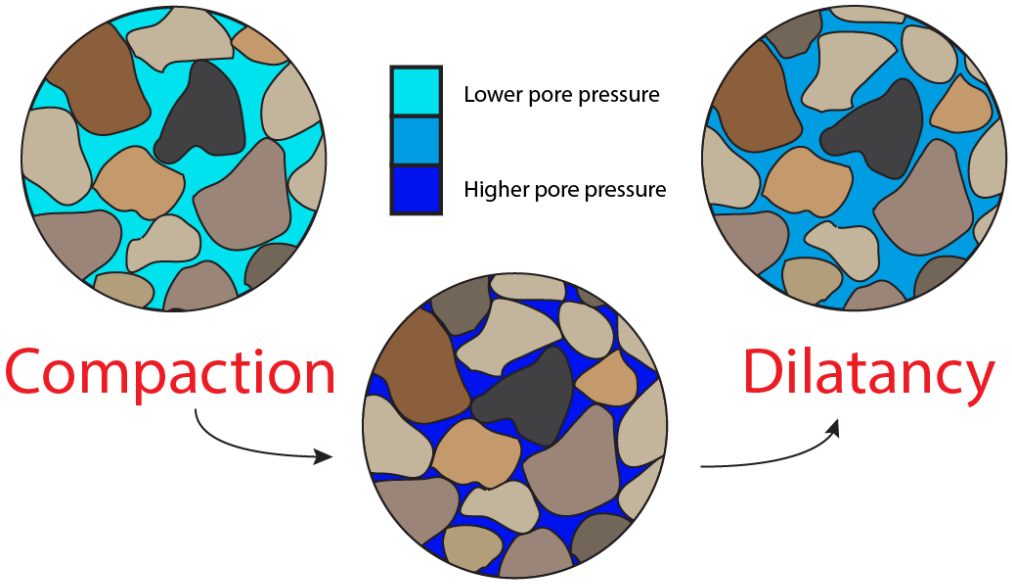

Compaction —*pore pressure increase*→ Weakening

Dilation —*pore pressure reduction*→ Strengthening

Finite Element Model: Geometry

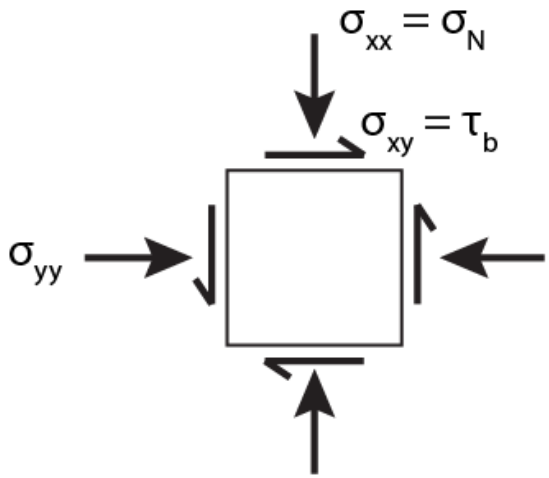

$\rho = 2670 \text{ kg/m}^3$

$V_P = 6000 \text{ m/s}$

$V_S = 3464 \text{ m/s}$

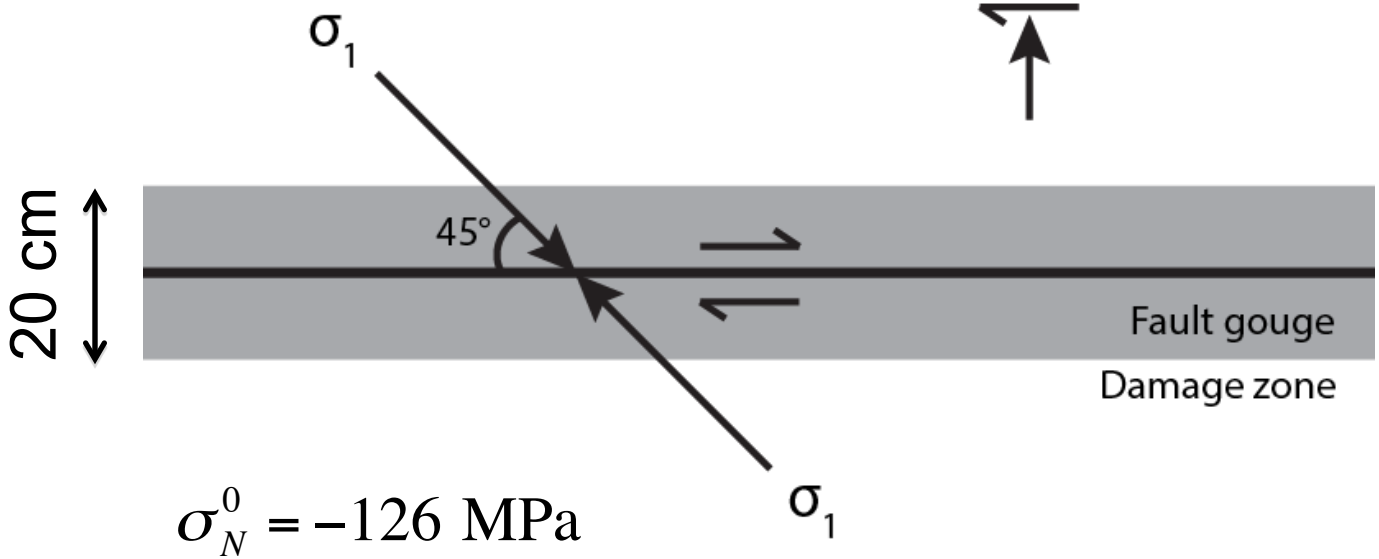

$\sigma_N^0 = -126 \text{ MPa}$

$\tau_b^0 = 35 \text{ MPa}$

$\tau_b^0 / \sigma_N^0 = 0.2778$

Element size: 1 cm

Rate-and-State Friction with Strongly Velocity-Weakening

$$f(V,\psi) = a\sinh^{-1}\left[\frac{V}{2V_0}\exp\left(\frac{\psi}{a}\right)\right],$$

State variable evolves via the slip law:

$$\dot{\psi} = -\frac{V}{L}(\psi - \psi_{ss}),$$

$$f_{ss} = f_w + (f_{LV} - f_w)\left[1 + \left(\frac{V}{V_w}\right)^8\right]^{-\frac{1}{8}},$$

$$\psi_{ss} = a\ln\left[\frac{2V_0}{V}\sinh\left(\frac{f_{ss}}{a}\right)\right].$$

$$f_{LV} = f_0 - (b-a)\ln\left(\frac{V}{V_0}\right),$$

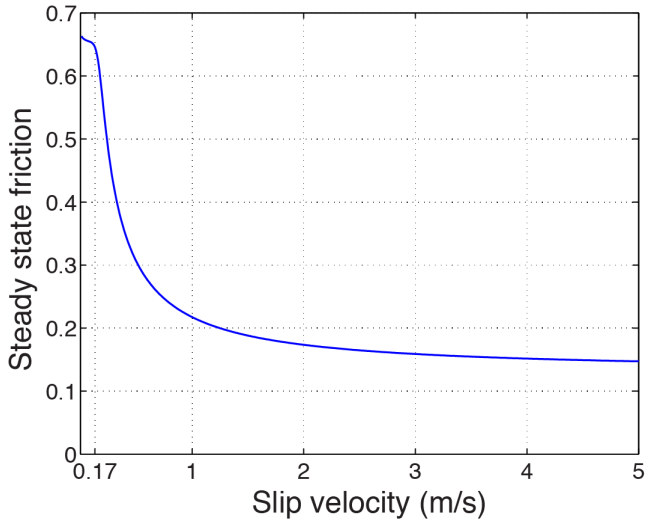

Direct effect parameter	a	0.016
State variable evolution parameter	b	0.2
State variable evolution distance	L	1.3717×10^{-4} m
Reference friction	f_0	0.7
Reference slip velocity	V_0	1.0 μm/s
Weakened friction coefficient	f_w	0.13
Weakening velocity	V_w	0.17 m/s

Constitutive Modeling

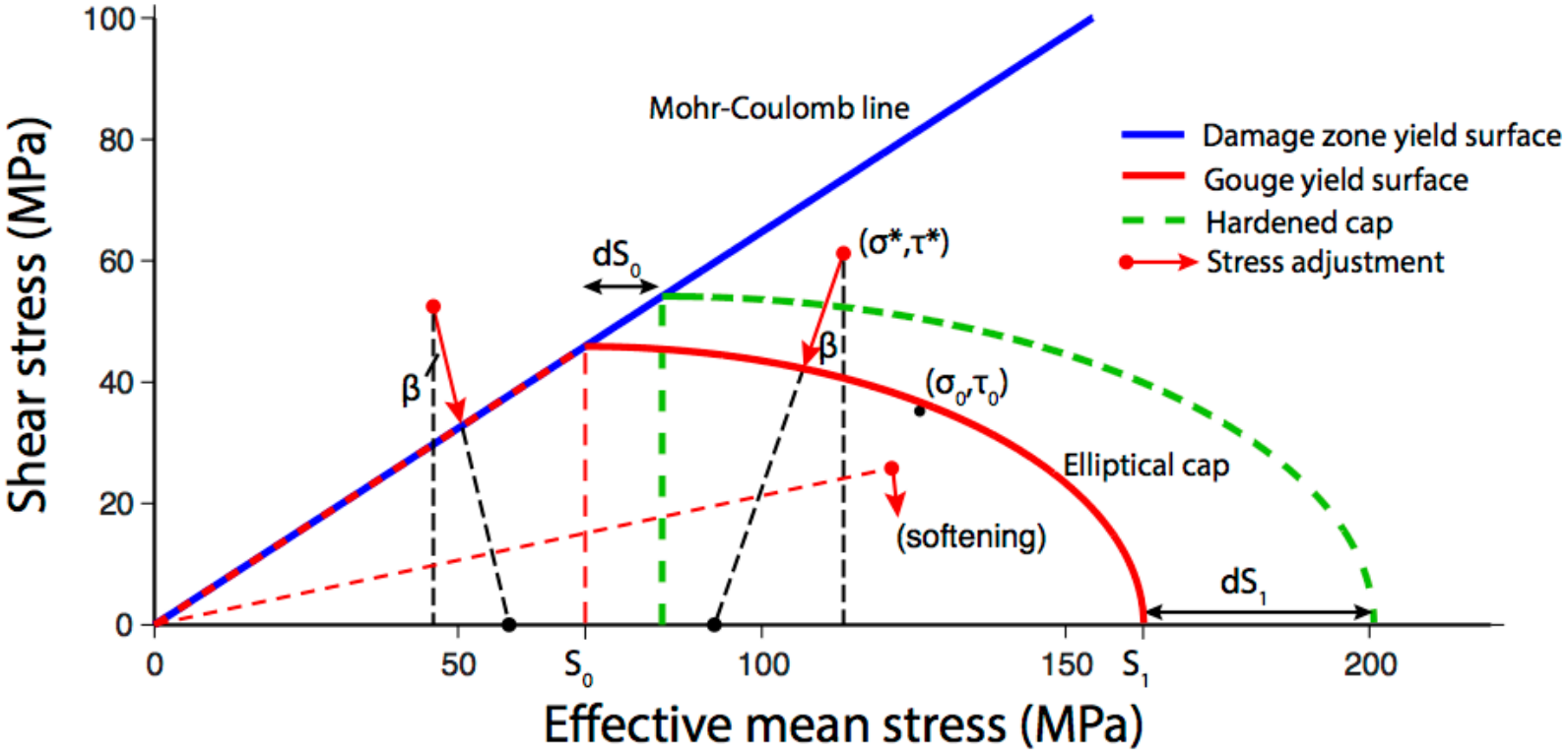

Mohr Coulomb yielding at low stress:

$$\tau = c + \mu\sigma$$

Elliptical cap at high stress:

$$\left(\frac{\sigma - S_0}{a}\right)^2 + \left(\frac{\tau}{b}\right)^2 = 1$$

Constitutive Modeling

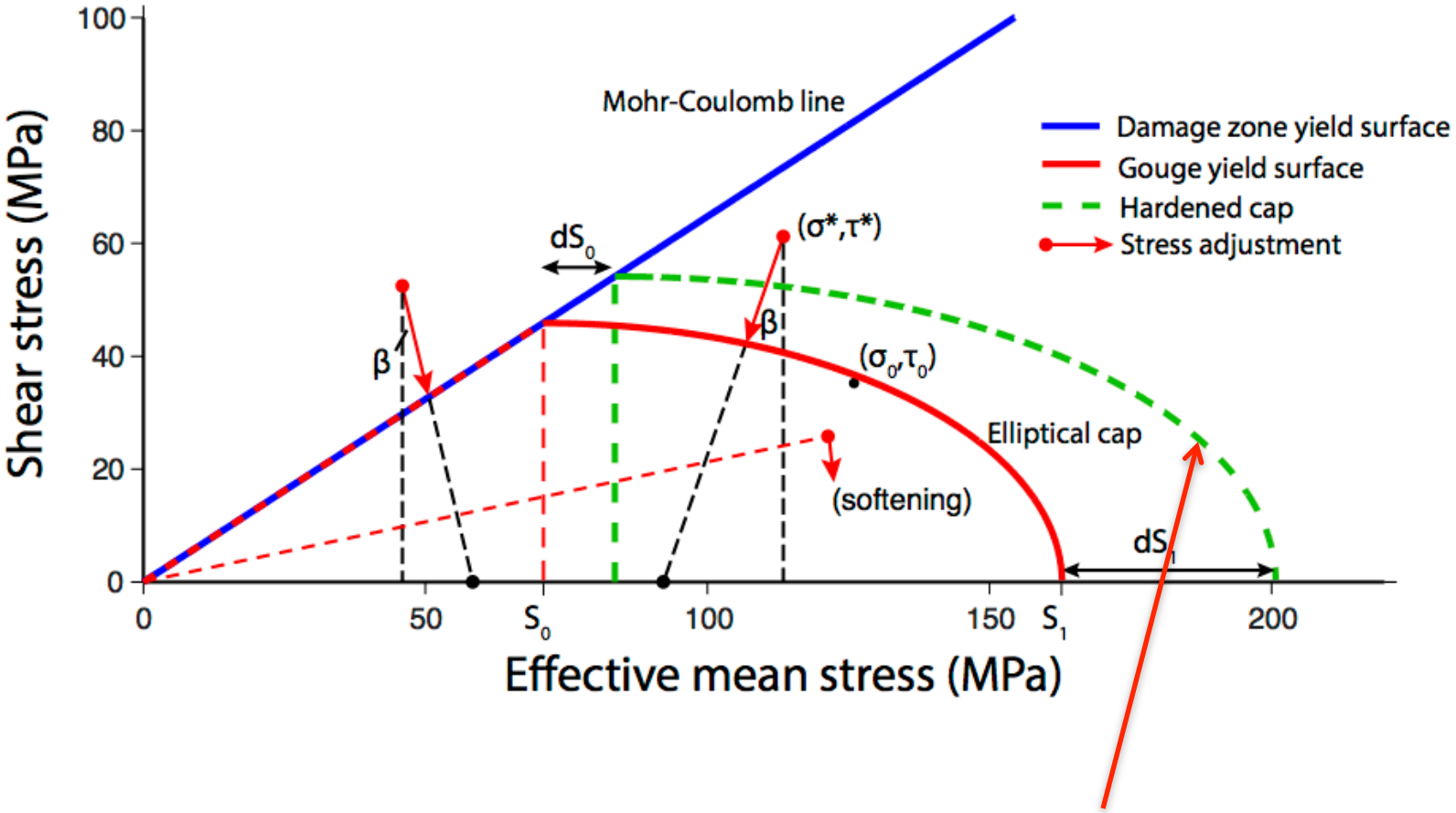

Hardening rule

$$dS_0 = 0.5\ K_{drained}\ (-d\varepsilon^p_{kk}) + 0.2\ G\ d\eta$$

η : inelastic shear strain

$$dS_1 = 3\ dS_0$$

Constitutive Modeling

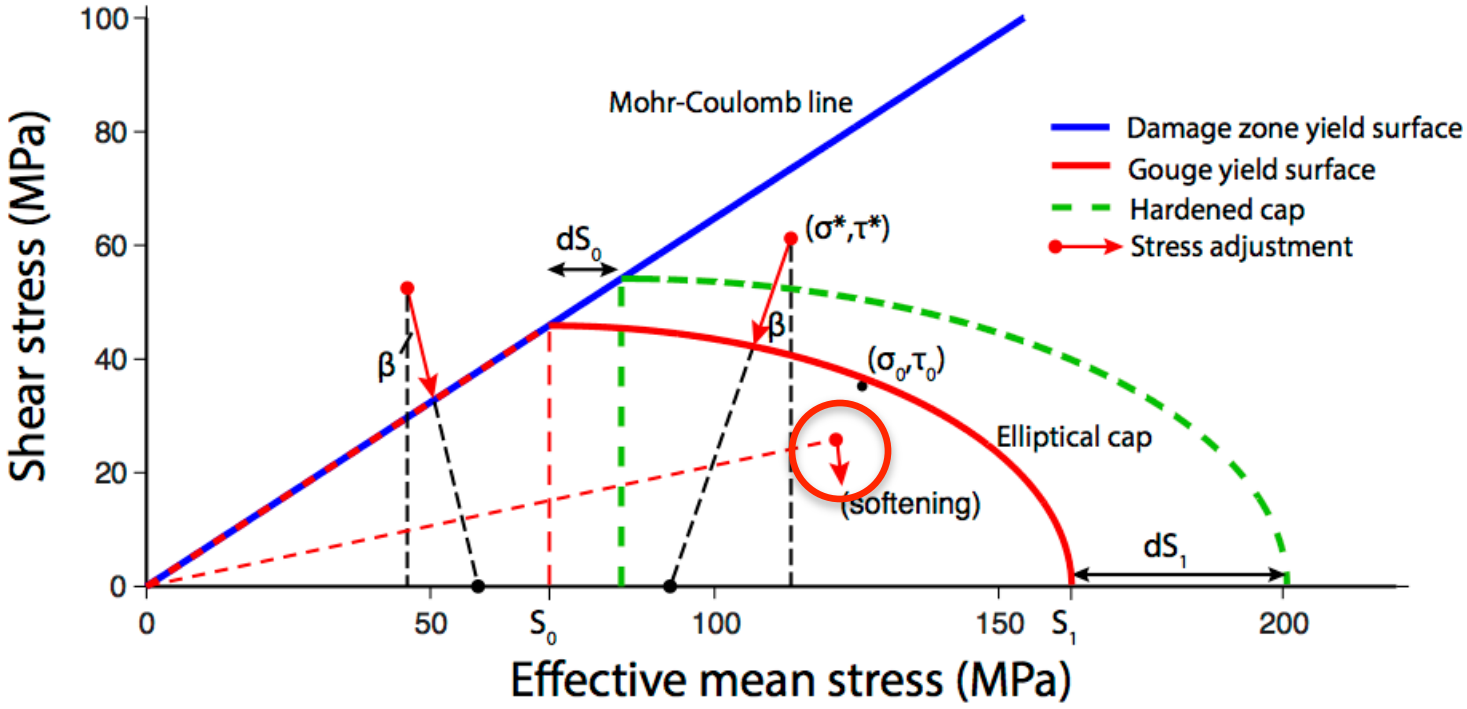

Dilatancy rule

$$\dot{\varepsilon}^{p}_{kk} = -\frac{V_{ev}}{L}(\varepsilon^{p}_{kk} - \varepsilon^{p,ss}_{kk})$$

$$\dot{\eta} = \tan\beta\ \dot{\varepsilon}^{p}_{kk}$$

$$\varepsilon^{p,ss}_{kk} = \zeta \sinh^{-1}\left(\frac{V_{ev}}{2V_0}\right)$$

$$V_{ev} = \xi V \exp\left(\frac{-x^2}{2s^2}\right)$$

- Simulates dilatancy of frictional surface

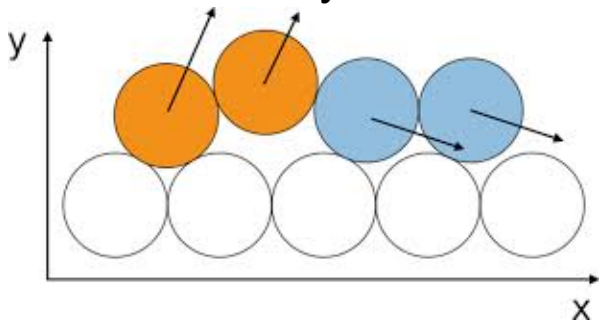

analogous to Segall and Rice's (1995) porosity evolution

Pore Pressure Change in Undrained Condition

$$\dot{p} = -B\frac{\dot{\sigma}_{kk}}{3} - \frac{KB}{\alpha}\dot{\varepsilon}^{p}_{kk}$$

Viesca et al. (2008)

elastic

inelastic

B: Skempton's coefficient (0.6)

K: drained bulk modulus

α : Biot's coefficient (0.45)

Pore pressure change on the Fault

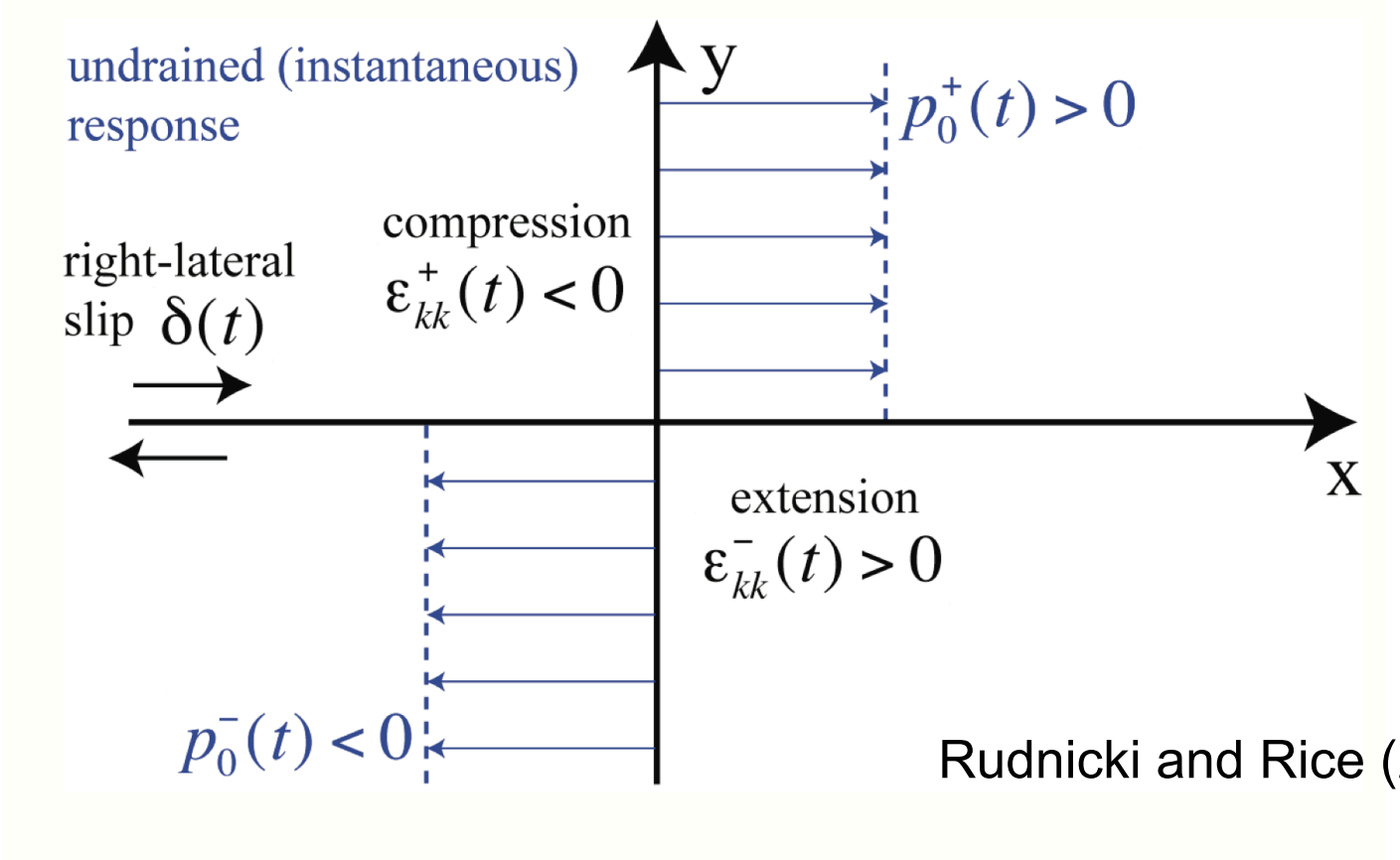

Rudnicki and Rice (2006)

We average the pore pressure changes on both sides of the fault (i.e., ignoring damage-induced poroelastic parameter changes)

Snapshot at t = 8 ms

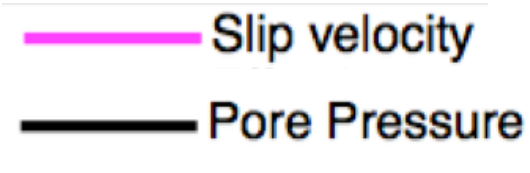

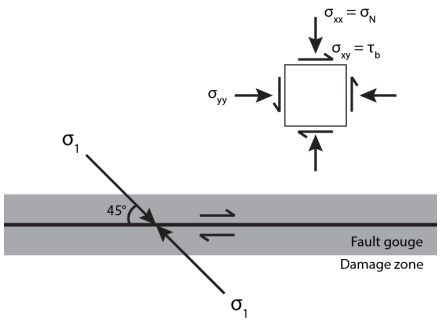

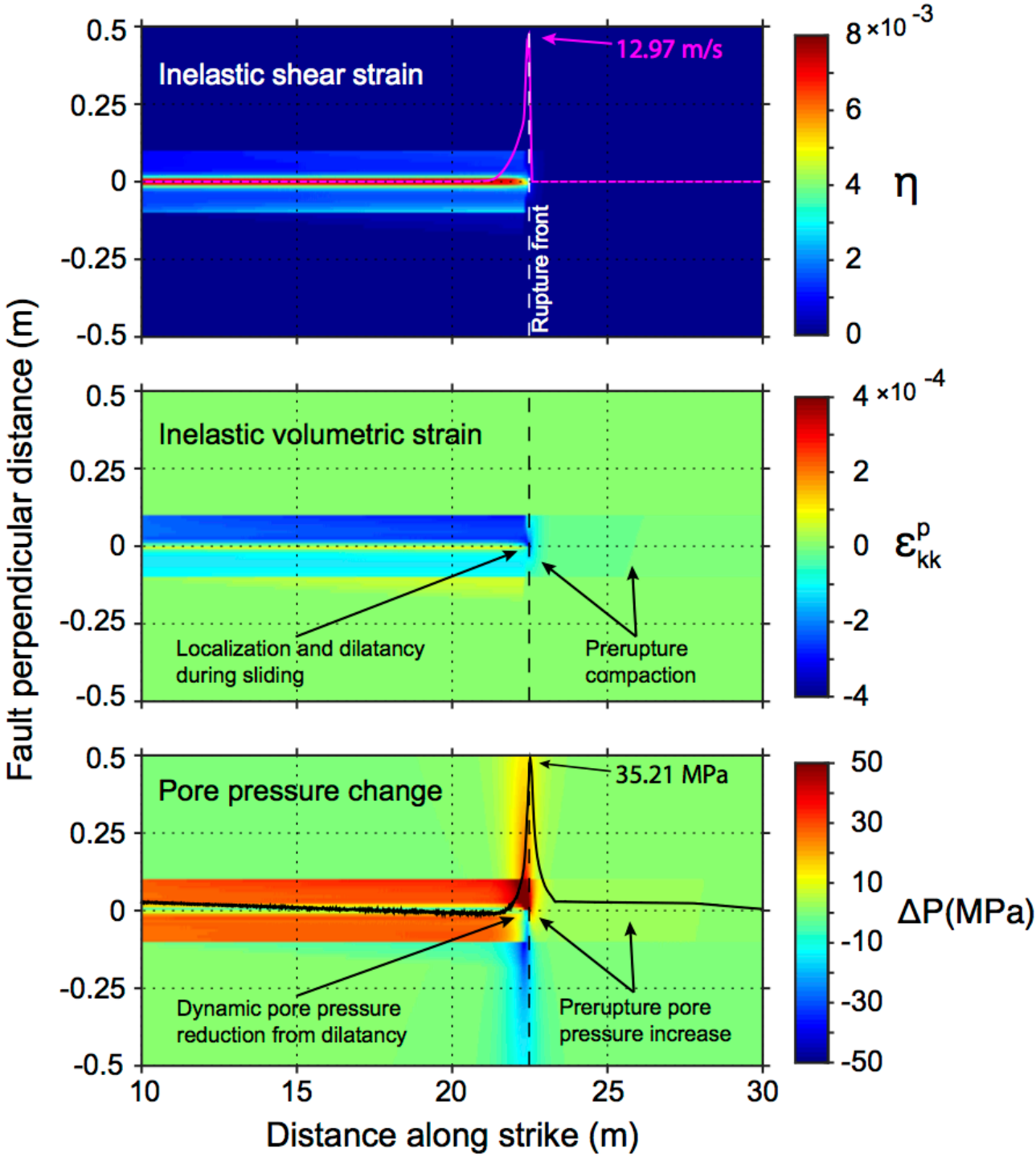

On-Fault Time Histories at 15 m from Hypocenter: Elastic vs. Inelastic

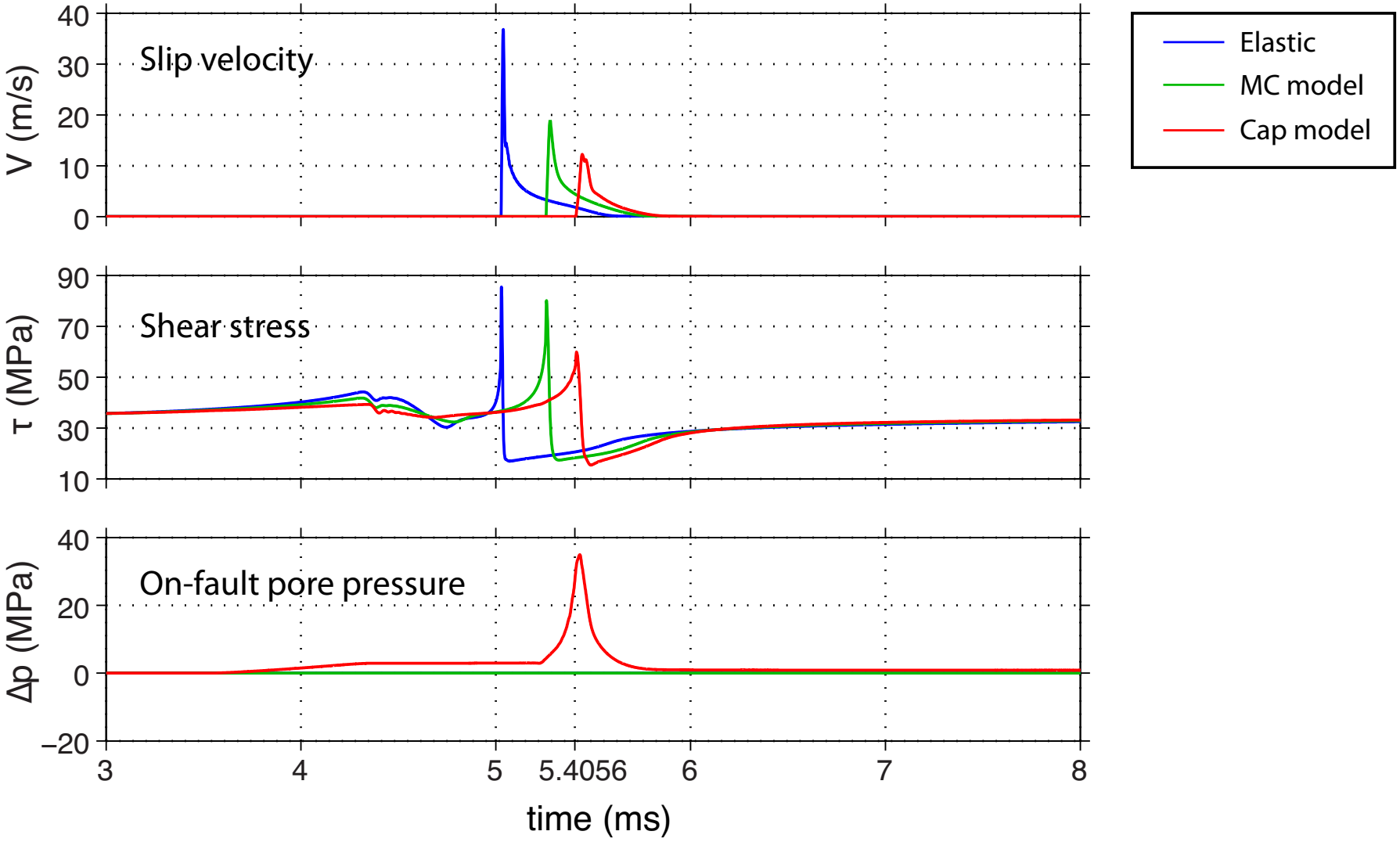

Effect of Dilatancy

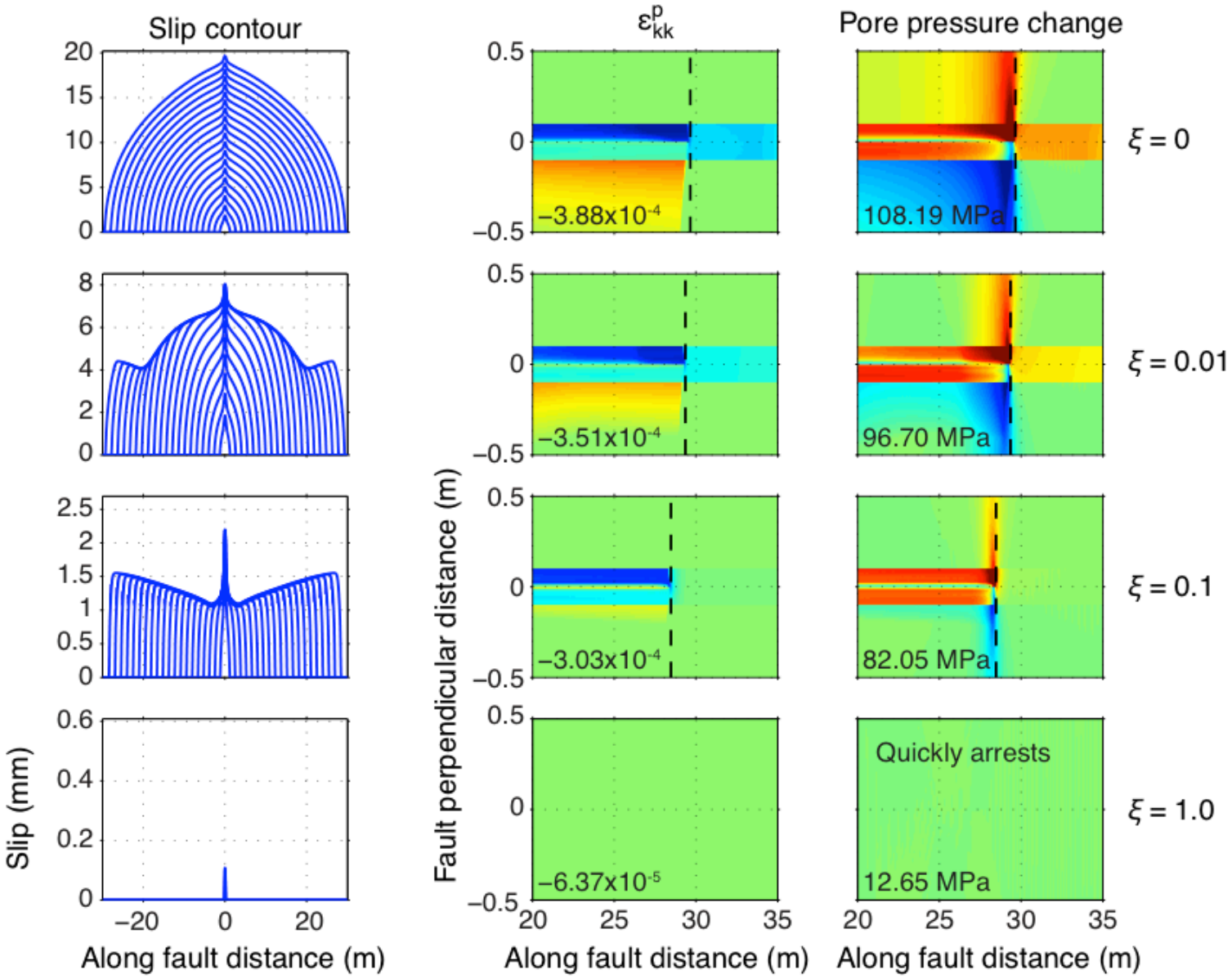

Self-Healing Slip Pulse

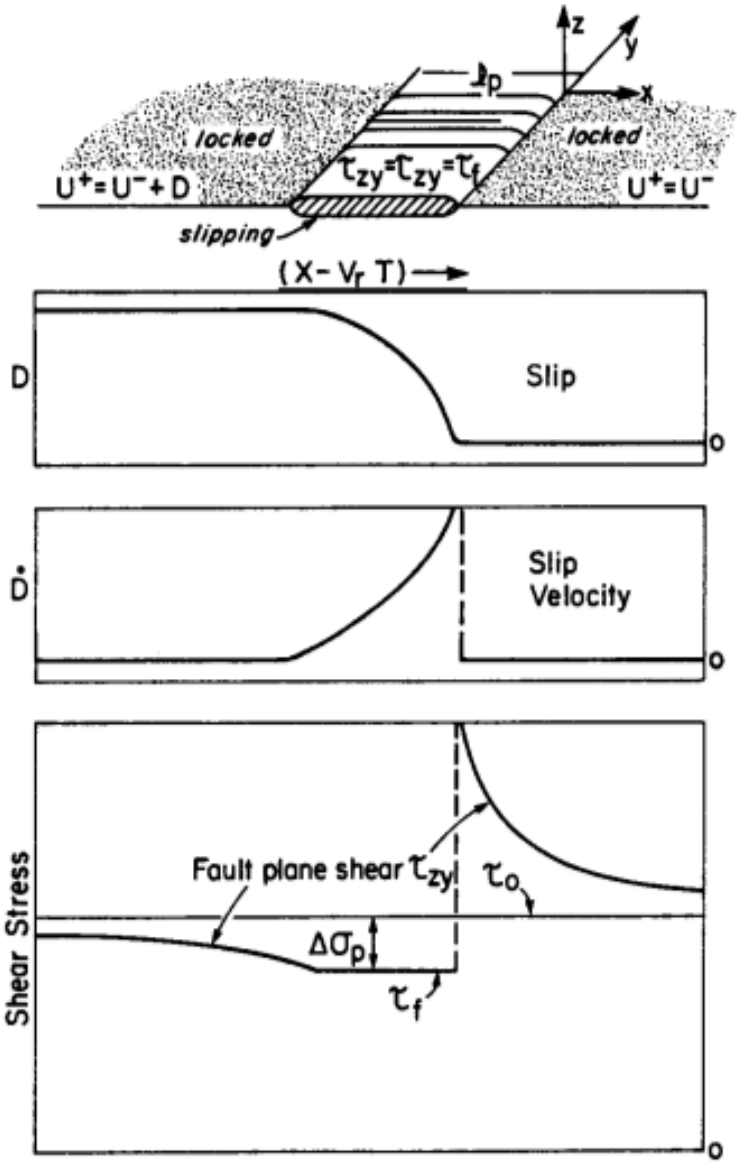

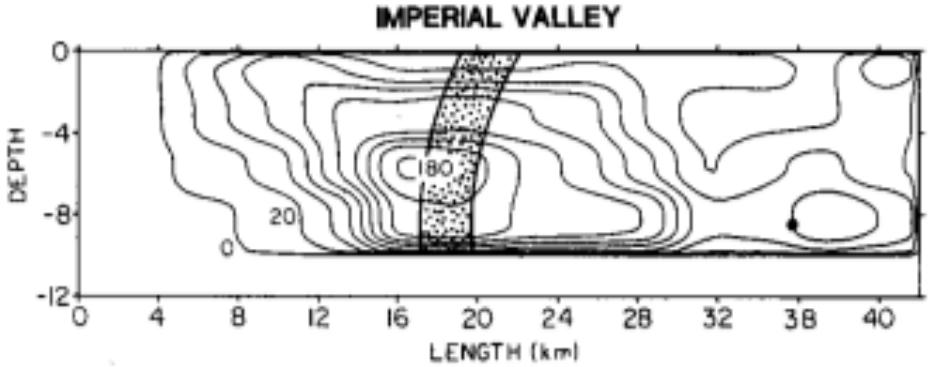

Fig. 5. Slip distribution (cm) for the $M = 6.2$ 1984 Morgan Hill, CA, earthquake derived by Hartzell and Heaton (1986) from the inversion of strong motion waveform data. The large dot denotes the hypocenter and the stippled region denotes the approximate region that is slipping at a particular instant in time.

From Heaton (1990)

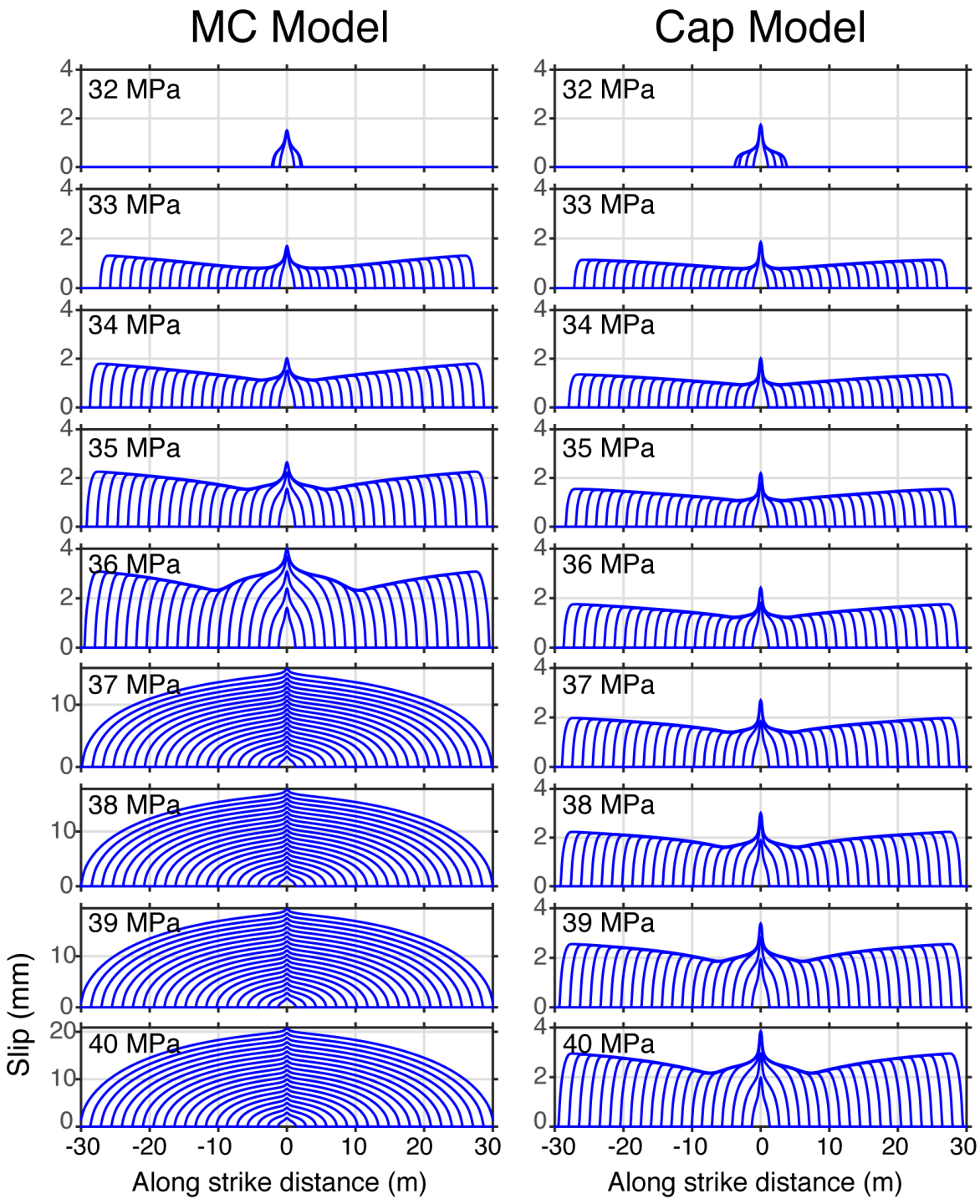

Effect of Background Shear Stress Level

(Slip contours are at 0.5 ms)

Strain localization in fault gouge

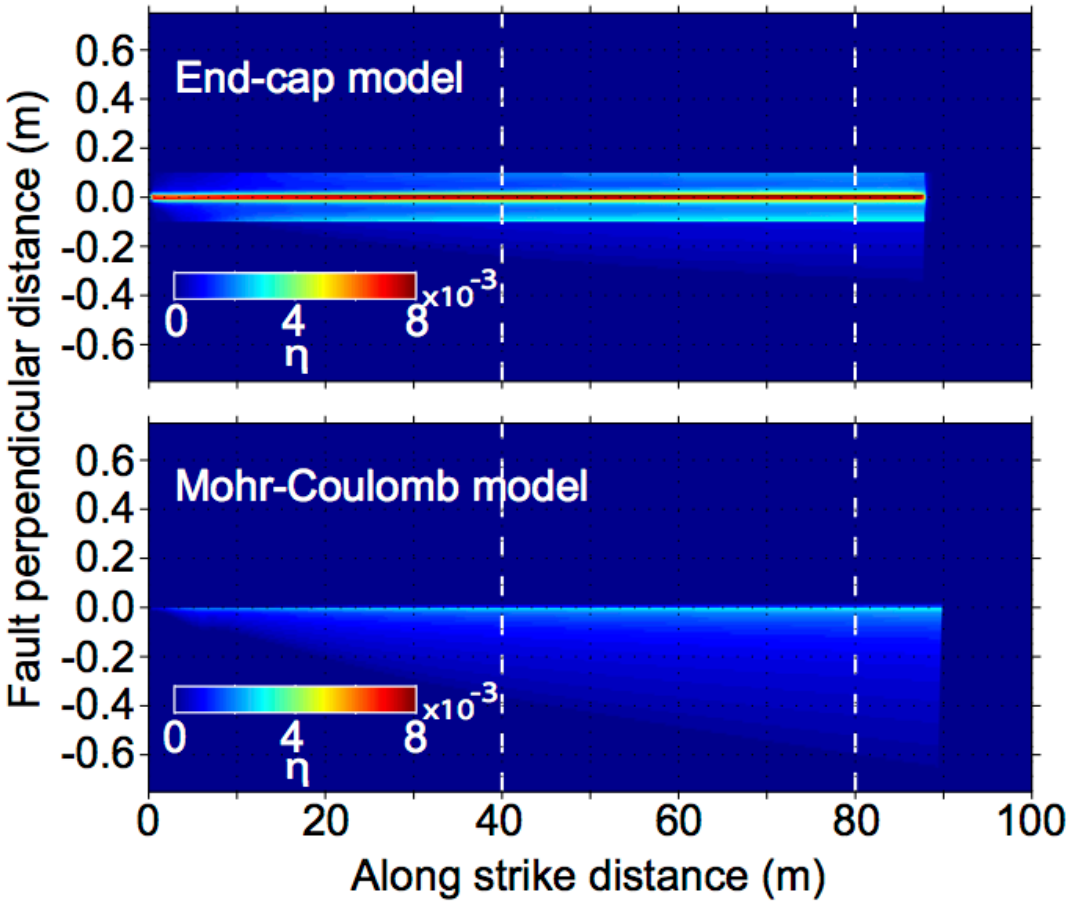

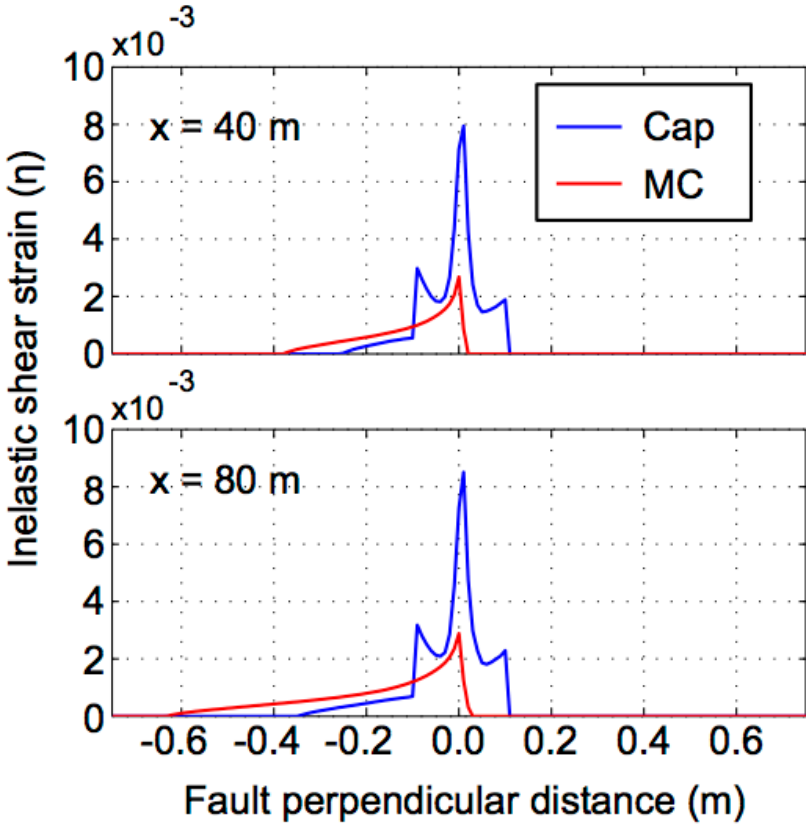

Conclusions

- The presence of well-developed fault gouge might explain the weakness of mature faults, such as the SAF.
- Gouge compaction due to large shear stress increase ahead of rupture front increases the pore pressure and reduces static friction, weakening the fault.
- Gouge dilation during stress breakdown reduces the pore pressure and strengthens the fault, promoting slip pulses.
- Rapid gouge dilatancy and softening during sliding highly localizes shear strain to the fault surface; reduction in strength drop leads to less plastic strain in the damage zone

Thank you!
Questions?